Journal Pre-proof

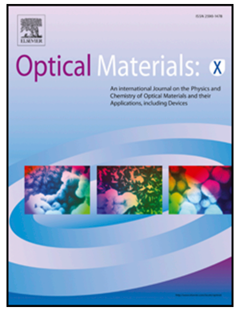

Fabrication of low loss channel waveguide in tungsten-tellurite glass by 11☐MeV carbon ion microbeam for telecom C band

István Bányász, Edit Szilágyi, Istvan Rajta, Gyula U.L. Nagy, Stefano Pelli, Gualtiero Nunzi Conti, Simone Berneschi, Vladimir Havránek, Vaclav Vosecek, Norbert Nagy, Zoltan Szabó, Miklos Veres, Adolfo Speghini

PII: S2590-1478(19)30032-4

DOI: https://doi.org/10.1016/j.omx.2019.100035

Reference: OMX 100035

To appear in: *Optical Materials: X*

Received Date: 15 July 2019

Revised Date: 17 August 2019

Accepted Date: 11 September 2019

Please cite this article as: Istvá. Bányász, E. Szilágyi, I. Rajta, G.U.L. Nagy, S. Pelli, G. Nunzi Conti, S. Berneschi, V. Havránek, V. Vosecek, N. Nagy, Z. Szabó, M. Veres, A. Speghini, Fabrication of low loss channel waveguide in tungsten-tellurite glass by 11☐MeV carbon ion microbeam for telecom C band, *Optical Materials: X* (2019), doi: https://doi.org/10.1016/j.omx.2019.100035.

Fabrication of Low Loss Channel Waveguide in Tungsten-Tellurite Glass by 11 MeV Carbon Ion Microbeam for Telecom C Band

István Bányász[a], Edit Szilágyi[a], Istvan Rajta[b], Gyula U.L. Nagy[b], Stefano Pelli[c*], Gualtiero Nunzi Conti[c], Simone Berneschi[c], Vladimir Havránek[d], Vaclav Vosecek[d], Norbert Nagy[e], Zoltan Szabó[e], Miklos Veres[f], Adolfo Speghini[c,g]

[a]Department of Nuclear Materials Science, Wigner Research Centre for Physics, Hungarian Academy of Sciences, P.O.B. 49, H-1525, Budapest, Hungary

[b]MTA Atomki, Institute for Nuclear Research, Hungarian Academy of Sciences, H-4001 Debrecen, P.O. Box 51, Hungary

[c]MDF-Lab, Institute of Applied Physics "Nello Carrara", IFAC-CNR, Via Madonna del Piano 10, I-50019 Sesto Fiorentino (FI), Italy

[d]Nuclear Physics Institute AV CR, Řež near Prague, 250 68, Czech Republic

[e]Institute for Technical Physics and Materials Science, Centre for Energy Research, Hungarian Academy of Sciences, Konkoly-Thege Rd. 29-33, 1121 Budapest, Hungary

[f]Department of Applied and Nonlinear Optics, Wigner Research Centre for Physics, Hungarian Academy of Sciences, P.O.B. 49, H-1525, Budapest, Hungary

[g]NRG - Department of Biotechnology, University of Verona, and INSTM, RU of Verona, Strada Le Grazie 15, I-37314 Verona, Italy

* s.pelli@ifac.cnr.it

Abstract: Channel waveguides were directly written in Er: $TeO_2W_2O_3$ glass using 11 MeV C^{4+} ion microbeam with fluences in the range of $1\cdot10^{14}$ - $5\cdot10^{16}$ ion/cm^2. The channel waveguides supported a single guided mode at λ= 1540 nm. Propagation losses of the as-irradiated channel waveguides were around 14 dB/cm. A 30-minute thermal annealing at 150 °C in air reduced propagation losses at λ = 1400 nm to 1.5 dB/cm. This method produced channel waveguides with confinement and propagation losses comparable to or better than other current methods, such as MeV energy focused proton or helium ion beam writing.

Keywords: Integrated optics, rare earth doped materials, channel waveguides, optical design and fabrication, microstructure fabrication.

1. Introduction

Optical waveguides are fundamental elements in modern telecommunications systems. A large number of optical crystals and glasses were identified as suitable optoelectronic materials. However, fabrication of waveguides in some of these materials remains still a challenge due to their susceptibility to mechanical or chemical damages during processing. Ion beam implantation is able to modify the optical properties of optical materials, such as polymers, glasses and crystals. Numerous practical applications exist, e.g. waveguides, special coatings, optical confinement of semiconductor lasers, impurity additions for lasing regions, fabrication of nonlinear optical elements, and production of photochromic layers [1], [2]. Based on their atomic number, the ions used in the ion implantation process fall into two main categories: light and heavy ions. Light ions like H^+ and He^+ with relatively low energies have been used to produce optical waveguides in different materials by ion implantation from the beginning until recently [3]-[5]. The first ion implanted waveguides were produced by Schineller *et al.* by proton implantation into fused silica glass in 1968 [6]. In this case, the main contribution to the formation of the guiding structure is generated by the nuclear damage produced by incoming ions during their track through the material.

Together with light ions, medium and high-mass ions (i.e.: Li^+, B^+, C^+, N^+, O^+, Na^+, Ar^+, Bi^+) were also used to modify the properties of materials [7]-[11]. In particular, if their energy is greater than 1 MeV/amu, these ions are referred to as "swift heavy" [2].

When mass and energy of the implanted ion are low, formation of adequate refractive index changes for waveguide fabrication requires relatively high fluencies, in the 10^{15} - 10^{17} ions/cm^2 range.

However, with higher ion mass and energy, the required fluence is at least an order of magnitude lower because the electronic interaction becomes high enough to change the optical properties of the materials..

First studies on the effects of swift heavy ion irradiation on the optical properties of materials date back to the 1990's [12].

Fabrication of slab waveguides with swift heavy and medium-light ions has been demonstrated in crystals and glasses alike. The refractive index change needed to fabricate an optical waveguide has been produced either by the electronic interaction between the ions and the target atoms or by the creation of an optical barrier at the stopping range of the ions [13] - [17].

In order to obtain channel waveguides by ion implantation, the needed patterning by selection of the irradiated area can obtained either by masking or by microbeam direct writing.

Vazquez et al. followed the former approach and obtained channel waveguides by carbon ions implantation in a soda lime Er^{3+}/Yb^{3+} doped glass [18]. Due their interest to upconversion, they demonstrated propagation only in the visible spectral interval.

Since the development of ion microbeam facilities attached to accelerators, proton microbeams have been used for producing channel waveguides and other microoptical elements in organic and inorganic optical materials [19]-[22]. Microbeam techniques offer the advantage of not needing the use of masks, thus significantly reducing the necessary steps to obtain a waveguide. Even more importantly, they add flexibility to the fabrication of components, since in order to test different design parameters no additional photolithographic masks have to be produced and only the maskless direct writing procedure is required.

Roberts and von Bibra tested their focused proton beam written buried channel waveguides in fused silica at visible wavelengths, obtaining propagation losses of about 0.5 dB/cm at λ=632.8 nm in their best channel waveguide [19]. Bettiol et al. fabricated buried channel waveguides in a Foturan™ photosensitive glass using 2 MeV focused proton beam. They achieved 8.3 dB/cm minimum propagation losses at λ=632.8 nm for a fluence of 10^{14} protons/cm^2 [20]. The same group produced erbium-doped waveguide amplifiers (EDWAs) in an IOG-1 Phosphate laser glass, co-doped with Er and Yb ions, via direct writing with a 2 MeV proton microbeam [21]. The best propagation loss they obtained after thermal annealing was around 0.8 dB/cm at λ =1300 nm, and highest net gain was 1.72 dB/cm, measured at λ =1534 nm with a pump beam at 975 nm. An et al. fabricated channel waveguides with proton beam implantation in chalcogenide glasses with $4 \cdot 10^{15}$-10^{16} cm^2 fluences and reaching 2 dB/cm propagation losses at 1.064 nm [22]. Yao et al. fabricated a Nd: YAG channel waveguide laser using also direct writing with a 1 MeV proton microbeam [23]. The losses of their channel waveguides were approximately 4 dB/cm.

Besides the above-mentioned previous art and based on our experience in fabrication/characterisation of planar waveguides in optical materials [24]-[26], in this paper we demonstrate the feasibility of fabricating channel waveguides in rare earth tungsten-tellurite glass directly by heavy ions microbeam implantation. We have assessed their main guided propagation and structural characteristics also as a function of a thermal annealing process.

The advantages and the novelty of the proposed method are to be found in the ease and simplicity of the writing process, which does not require any intermediate photolithographic step and/or the use of any mask, as well as in the reduction of the irradiation time (i.e.: that of a final device production time) thanks to the higher energy and low fluence values made available by a modern Tandetron.

The channel waveguides so obtained are single mode at the telecom C band and the propagation losses are comparable to or better than other current methods, such as MeV energy focused proton or helium ion beam writing. The achievement of this important result represents the starting point for the development of any integrated device by swift heavy ions (C^{4+} ions in our case) microbeam technique.

Experiments and results

Er^{3+} doped tellurite glass with $60TeO_2$-$25WO_3$-$15Na_2O$-$0.5Er_2O_3$ (mol. %) composition was prepared by melt-quenching technique [26]. Fabrication of the channel waveguides was carried out at the 3 MV Tandetron 4130 MC (High Voltage Engineering Europa B.V.) of the Nuclear Physics Institute AV CR, Řež. Channel waveguides were directly written in the sample with a microbeam of 11 MeV C^{4+} ions. Beam current was in the 4-6 nA range. The microbeam size for the channel waveguides was 8 µm x 12 µm, the shorter side being the width of the channel waveguides. Channel waveguides were written by scanning the target stage under the stationary microbeam. Irradiated fluence was controlled by the velocity of the stage scan. The length of the channel waveguides was 9 mm. Irradiated fluences ranged from $1\cdot10^{14}$ to $5\cdot10^{16}$ ions/cm^2.

Nuclear and electronic energy losses vs. sample depth were calculated using the DEPTH code [28] and the ZBL'95 set of stopping powers [29]. The results are presented in Fig. 1. Energy loss due to electronic interaction increases slowly until reaching a maximum at 3.8 µm then decreases more rapidly. Energy loss produced by nuclear interaction has a sharp peak at 6.9 µm. We point out that the maximum of the electronic energy loss is about 15 times higher than that of the nuclear one. According to the models developed by Olivares et al. [17], irradiation with swift heavy ions of low fluence creates a partially amorphised layer with reduced refractive index around the broad peak of the electronic loss, acting as an optical barrier and allowing for guiding of light between that layer and the substrate surface.

The irradiated channel waveguides were first examined by interference phase contrast (INTERPHAKO) microscopy to assess in particular the homogeneity of the fabricated structures. In Fig. 2 we report the image of portion of four channel waveguides.

The ability of propagating modes of each channel waveguide was tested at λ = 1540 nm and insertion losses were measured at 1400 nm, outside the absorption band of Er^{3+} [30]. The bottom channel waveguide in Fig. 2 proved to be the best one. Coupling and propagation losses were assessed by measuring the light intensity at the exit edge of the waveguides by following a well-established procedure as described in detail in [31], [32].

Measured as-implanted, net propagation losses of all the channel waveguides were in the range 14-20 dB/cm. The channel waveguide irradiated with a fluence of $4.6\cdot10^{14}$ ion/cm^2 presented the lowest propagation loss, 14 dB/cm. These high losses would make the as-implanted channel waveguides useless for practical purposes.

Based on our previous experiences with ion-implanted slab waveguides in the same material [33], we applied stepwise thermal annealing to the sample, and measured the propagation losses of the best as-implanted waveguide after each annealing step.

Results of a stepwise thermal annealing sequence for the best waveguide (lowermost waveguide in Fig. 2) are presented in Fig. 3.

A moderate 30 minutes thermal annealing at 150 °C in air caused a significant improvement of the guiding properties of the channel waveguide. As it can be seen in Fig. 3, propagation losses measured at λ = 1400 nm were 14 dB/cm in the as-implanted channel waveguide. They decreased to 1.5 dB/cm after the 150 °C thermal annealing. Further stepwise thermal annealing up to 300 °C resulted in increasing propagation losses, though an improvement in coupling losses was measured after the annealing step at 200 °C. The latter accounted for the improvement of insertion losses to their minimum value at 200-250 °C. Further increase of the annealing temperature caused a general worsening of the guiding capability of the waveguide, also testified by the increase in the horizontal dimension of the guided mode for the annealing at 300 °C, other than the higher coupling and propagation losses.

Near field image of the emerging beam at the output face of that channel waveguide after a thermal annealing step at 150 °C is shown in Fig. 4. The image has been captured by focusing with a 10X microscope objective the output light beam generated by an Anritsu Reference ES ECL tuneable laser source (1400 nm, 4 mW CW) on the sensor of a C1000 Hamamatsu Vidicon camera. The data have been corrected against the nonlinear response of the camera. The waveguide is monomode in both transversal directions, but the mode extends well beyond the estimated transversal physical dimensions of the waveguide.

Fig. 5 shows the mode dimensions measured from the near field images (I_{MAX}/e^2 intensity threshold, I_{MAX} being the maximum intensity of the mode). The mode width does not vary significantly with the temperature, until the 300 °C annealing step, when the mode structure deteriorates significantly. The estimated depth of the waveguides shows a slight increase when successive annealing steps are applied.

While propagation losses could be reduced by thermal annealing, and depth confinement of the focused ion beam written channel waveguides was good, it was noticed that lateral confinement in the channel was not optimal, because of the small refractive index contrast between the waveguide core and the not implanted bulk material at both sides. This is the reason for the significant difference between the mode diameter and the physical dimension of the beam and its impact on the glass structure, as measured also by our Raman measurements.

Besides of transmission optical microscopy, the ion beam written channel waveguides were also studied by profilometry (Bruker Dektak XT, tip radius: 5 μm) to check for possible surface relief structures. Surface profiles over three channel waveguides taken after the stepwise thermal annealing are shown in Fig. 6. Amplitudes of the ridges are about 110 nm for the bottom channel in Fig. 2 (F=4.6 $\cdot 10^{14}$ ion/cm^2) and about 70 – 80 nm for the two channels above it (F=1.4 $\cdot 10^{14}$ ion/cm^2 for both). Note the presence of two deep and narrow trenches on both sides of the bottom channel waveguide. They can be attributed to the strain caused by the high temperature difference at the edge of channel waveguide during irradiation [34-36].

The heights of the ridges are too small to support light propagation by themselves, which must therefore be ascribed to the refractive index changes induced in the glass by the ion irradiation.

To obtain information on the structural changes produced by the ion microbeam irradiation in the channel waveguides, micro Raman spectroscopy was performed with a Renishaw 1000 micro Raman spectrometer. Excitation wavelength was 785 nm. Both full width at half-maximum (FWHM) and peak position of the Raman lines changed in the irradiated regions. Full width at half maximum (FWHM) of a 922.3 cm^{-1} Raman line across two channel waveguides, irradiated with a carbon microbeam of E=1 MeV at fluences of 4.6$\cdot 10^{14}$ ion/cm^2 (*implanted and annealed*) is presented in Fig. 7.

The decrease in FWHM of the Raman peak in the irradiated region indicates transformation and some ordering of the glassy network.

Peak position of the 922.3 cm^{-1} Raman line across the same channel waveguide was also extracted from the Raman spectra. Raman peak positions are usually affected by the internal stress of the structure, causing bond length and bond angle distortions. Higher internal stress causes shift of the Raman peak to higher wavenumbers. It was found that amplitude of the variation of the peak position of the Raman line across the channel waveguide was about 1.1 cm^{-1}.

2. Conclusions

A novel method, i.e. direct writing with high-energy focused microbeam of medium-mass ions at low fluences, has been devised and realized for the fabrication of optical channel waveguides. The lowest propagation loss in a Er^{3+} doped tungsten-tellurite glass waveguide, measured at a wavelength of 1400 nm after a 30 minute thermal annealing at 150 °C, was 1.5 dB/cm. Due to the predominant electronic interaction, a fluence of 4.6$\cdot 10^{14}$ ion/cm^2, more than an order of magnitude lower than those applied in low-energy implantation, was sufficient for effective waveguide formation. The channel waveguides were formed immediately below the sample surface, in contrast to proton beam writing where deeply buried channel waveguides can be produced. The surface profilometry measurements revealed that ridges of amplitudes between 70 and 100 nm were formed above the channel waveguides.

The low losses of the fabricated waveguides open the use of this technique to test the fabrication of planar guided optical amplifiers and lasers in materials such as tellurite glasses where it can be difficult to use other techniques such as ion-exchange.

3. Acknowledgments

Part of this research has been carried out at the CANAM (Centre of Accelerators and Nuclear Analytical Methods) infrastructure LM 2015056. This publication was supported by the Hungarian Scientific Research Fund (OTKA K101223 and K108366), the OP RDE, MEYS, and Czech Republic under the project CANAM OP, CZ.02.1.01/0.0/0.0/16_013/0001812.

S. Berneschi acknowledges the European Community and the Tuscany Region for their funding within the framework of the SAFE WATER project (European Union's Horizon 2020 Research & Innovation program and the ERA-NET "PhotonicSensing" cofund - G.A. No 688735).

I. Bányász acknowledges The Italian Research Council (CNR) for its funding in the Short Term Mobility Project 2016, under contract number Prot. AMMCNT-CNR n. 54178.

A. Speghini thanks University of Verona, Verona, Italy for financial support in the framework of "Ricerca di Base 2015" project.

References

[1] P.D. Townsend, P.J. Chandler and Zhang, L., Optical Effects of Ion Implantation, Cambridge University Press, Cambridge, 1994.

[2] F. Chen, Micro- and submicrometric waveguiding structures in optical crystals produced by ion beams for photonic applications, Laser & Photon Rev, 6 (2012) 622-640. https://doi.org/10.1002/lpor.201100037.

[3] G.L. Destefanis, P.D. Townsend, J.P. Gaillard, Optical waveguides in $LiNbO_3$ formed by ion implantation of helium, Appl. Phys. Lett. 32 (1978), 293-294. https://doi.org/10.1063/1.90025.

[4] S.M. Mahdavi, P.J. Chandler, P.D. Townsend, Formation of planar waveguides in bismuth germanate by $^4He^+$ ion implantation, J. Phys. D App.l Phys. 22 (1989), 1354-1357. https://doi.org/10.1088/0022-3727/22/9/017.

[5] T.C. Sum, A.A. Bettiol, H.L. Seng, I. Rajta, J.A. van Kan, F. Watt, Proton beam writing of passive waveguides in PMMA, Nuclear Instruments and Methods in Physics Research B 210 (2003), 266-271. https://doi.org/10.1016/S0168-583X(03)01028-0.

[6] E.R. Schineller, R.P. Flam, D.W. Wilmot, Optical Waveguides Formed by Proton Irradiation of Fused Silica, J. Opt. Soc. Am. 58 (1968),1171-1176. https://doi.org/10.1364/JOSA.58.001171.

[7] A.P. Webb, P.D. Townsend, Refractive index profiles induced by ion implantation into silica, J. Phys. D Appl. Phys. 9 (1976), 1343-1354. https://doi.org/10.1088/0022-3727/9/9/011.

[8] P. Mazzoldi, Properties of ion implanted glasses, Nuclear Instruments and Methods in Physics Research 209-210 (1983), 1089–1098. https://doi.org/10.1016/0167-5087(83)90924-9.

[9] Jin-Hua Zhao, Xiu-Hong Liu, Qing Huang, Peng Liu, Lei Wang, Xue-Lin Wang, The array waveguides formed in $LiNbO_3$ crystal by oxygen-ion implantation, Nuclear Instruments and Methods in Physics Research Section B Beam Interactions with Materials and Atoms 268 (2010), 2923-2925. https://doi.org/10.1016/j.nimb.2010.05.009

[10] G.B. Montanari, P. De Nicola, S. Sugliani, A. Menin, A. Parini, A. Nubile, G. Bellanca, M. Chiarini, M. Bianconi, G.G. Bentini, Step-index optical waveguide produced by multistep ion implantation in $LiNbO_3$, Opt. Express 20 (2012), 4444-4453. https://doi.org/10.1364/OE.20.004444.

[11] Chun-Xiao, L., Jun, X., Xiao-Li, X., Shu, W., Wei, W., Hai-Tao, G., Wei-Nan, L., Bo, P., 2014. Oxygen-implanted optical planar waveguides in Er^{3+}/Yb^{3+}-codoped silicate glasses for integrated laser generation, Opt. Eng. 53, 037101. https://doi.org/10.1117/1.OE.53.3.037101.

[12] P. Sreeramana Aithal, H.S. Nagaraja, P. Mohan Rao, D.K. Avasthi, Asati Sarma, Effect of high energy ion irradiation on electrical and optical properties of para-hydroxy acetophenone, J. Appl. Physics 81 (1997), 7526. https://doi.org/10.1063/1.365294.

[13] G. Szenes, Ion-velocity-dependent track formation in yttrium iron garnet: A thermal-spike analysis, Phys. Rev. B 52 (1995), 6154-6157. https://doi.org/10.1103/PhysRevB.52.6154.

[14] G.G. Bentini, M. Bianconi, L. Correa, M. Chiarini, P. Mazzoldi, C. Sada, N. Argiolas, M. Bazzan, R. Guzzi, Damage effects produced in the near-surface region of x-cut $LiNbO_3$ by low dose, high energy implantation of nitrogen, oxygen, and fluorine ions, J. Appl. Physics 96 (2004), 242-247. https://doi.org/10.1063/1.1756219.

[15] Q.-F. Zhu, X.-L. Shen, R.-L. Zheng, P. Lv, H.-T. Guo, W.-N. Li, C.-X. Liu, Waveguiding structures in Yb^{3+}-doped phosphate glasses by double-energy proton and single-energy carbon-ion implantations, Mater. Res. Express 5 (2018) 016404. https://doi.org/10.1088/2053-1591/aaa1f7.

[16] Y. Wang, J. Zhao, Q. Zhu, J. Shen, Z. Wang, H.-T. Guo, C. Liu, Near-infrared carbon-implanted waveguides in $Tb3^{+}$-doped aluminum borosilicate glasses, Front. Optoelectron. (2019). https://doi.org/10.1007/s12200-019-0869-6.

[17] J. Olivares, G. García, A. García-Navarro, F. Agulló-López, O. Caballero, A. García-Cabañes, Generation of high-confinement step-like optical waveguides in $LiNbO_3$ by swift heavy ion-beam irradiation, Appl. Phys. Lett. 86 (2005), 183501. https://doi.org/10.1063/1.1922082.

[18] G.V. Vázquez, R. Valiente, S. Gómez-Salces, E. Flores-Romero, J. Rickards, R. Trejo-Luna, Carbon implanted waveguides in soda lime glass doped with Yb^{3+} and Er^{3+} for visible light emission, Optics & Laser Technology 79 (2016). http://dx.doi.org/10.1016/j.optlastec.2015.12.002

[19] A. Roberts, M.L. von Bibra, Fabrication of Buried Channel Waveguides in Fused Silica Using Focused MeV Proton Beam Irradiation, J. Lightw. Technol. 14 (1996), 2554-2557. https://doi.org/10.1109/50.548154.

[20] A.A. Bettiol, S.V. Rao, E.J. Teo, J.A. van Kan, F. Watt, Fabrication of buried channel waveguides in photosensitive glass using proton beam writing, Appl. Phys. Lett. 88 (2006), 171106. https://doi.org/10.1063/1.2198798.

[21] K. Liu, E.Y.B. Pun, T.C. Sum, A.A. Bettiol, J.A. van Kan, F. Watt., Erbium-doped waveguide amplifiers fabricated using focused proton beam writing, Appl. Phys. Lett. 84 (2004), 684–686. https://doi.org/10.1063/1.1644922.

[22] Q. An, C. Cheng, S. K. Vanga, A. A. Bettiol, F. Chen, Proton Beam Writing of Chalcogenide Glass: A New Approach for Fabrication of Channel Waveguides at Telecommunication O and C Bands, J. of Lightwave Technology 32 (2014), 4365-4369. https://doi.org/10.1109/JLT.2014.2354239.

[23] Y. Yao, Y. Tan, N. Dong, F. Chen, A.A. Bettiol, Continuous wave Nd: YAG channel waveguide laser produced by focused proton beam writing, Opt. Express 18 (2010), 24516-2452.1 https://doi.org/10.1364/OE.18.024516.

[24] S. Berneschi, G. Nunzi Conti, I. Bányász, A. Watterich, N.Q. Khanh, M. Fried, F. Pászti, M. Brenci, S. Pelli, G.C. Righini, Ion beam irradiated channel waveguides in Er^{3+}-doped tellurite glass, Appl. Phys. Lett. 90 (2007), 121136. https://doi.org/10.1063/1.2717085.

[25] I. Bányász, S. Berneschi, M. Bettinelli, M. Brenci, M. Fried, N.Q. Khanh, T. Lohner, G. Nunzi Conti, S. Pelli, P. Petrik, G.C. Righini, A. Speghini, A. Watterich, Z. Zolnai, MeV energy N^{+} -implanted planar optical waveguides in Er-doped tungsten-tellurite glass operating at 1.55 µm, IEEE Photonics J 4 (2012), 721-727. https://doi.org/10.1109/JPHOT.2012.2194997.

[26] I. Bányász, S. Berneschi, N.Q. Khánh, T. Lohner, K. Lengyel, M. Fried, Á. Péter, P. Petrik, Z. Zolnai, A. Watterich, G. Nunzi Conti, S. Pelli, G.C. Righini, Formation of slab waveguides in eulytine type BGO and CaF_2 crystals by implantation of MeV nitrogen ions, Nuclear Instruments and Methods in Physics Research Section B Beam Interactions with Materials and Atoms 286 (2012), 80–84. https://doi.org/10.1016/j.nimb.2011.12.039.

[27] G. Nunzi Conti, S. Berneschi, M. Bettinelli, M. Brenci, B. Chen, S. Pelli, A. Speghini, G.C. Righini, J. Non-Cryst. Solids, Erbium-doped silicate glasses for integrated optical amplifiers and lasers, 345&346 (2004), 343–348. https://doi.org/10.1016/j.jnoncrysol.2004.08.046.

[28] E. Szilágyi, F. Pászti, “Theoretical calculation of the depth resolution of IBA methods”, Nuclear Instruments and Methods in Physics Research Section B Beam Interactions with Materials and Atoms, 85 (1994), 616-620. https://doi.org/10.1016/0168-583X(94)95893-9.

[29] J.F. Ziegler, J.P. Biersack, SRIM – The stopping and range of ions in matter, Nuclear Instruments and Methods in Physics Research Section B, 268 (2010), 1818-1823. https://doi.org/10.1016/j.nimb.2010.02.091.

[30] S. Berneschi, M. Brenci, G. Nunzi Conti, S. Pelli, G.C. Righini, I. Bányász, A. Watterich, N.Q. Khanh, M. Fried, F. Pászti, Channel waveguides fabrication in Er^{3+}-doped tellurite glass by ion beam irradiation, Proc. SPIE 6475, (2007), 647509, https://doi.org/10.1117/12.702085.

[31] W.J. Wang, S. Honkanen, S.I. Najafi, A. Tervonen, Loss characteristics of potassium and silver double-ion-exchanged glass waveguides, J. Appl. Phys. 74 (1993), 1529-1533. https://doi.org/10.1063/1.354852.

[32] R. J. Deri, N. Yasuoka, M. Makiuchi, A. Kuramata, O. Wada, Efficient fiber coupling to low-loss diluted multiple quantum well optical waveguides, Appl. Phys. Lett. 55 (1989), 1495-1497. https://doi.org/10.1063/1.101588.

[33] S. Berneschi, I. Cacciari, G. Nunzi Conti, S. Pelli, G.C. Righini, I. Bányász, N.Q. Khanh, T. Lohner, P. Petrik, Z. Zolnai, M. Bettinelli, A. Speghini, L. Mescia, F. Prudenzano, Annealing effect on optical barrier in ion-implanted tellurite glass waveguides, Proc. SPIE 7218 (2009), 72180. https://doi.org/10.1117/12.811153.

[34] H. Trinkaus, A. I. Ryazanov, Viscoelastic Model for the Plastic Flow of Amorphous Solids under Energetic Ion Bombardment, Phys. Rev. Lett. 74 (1995), 5072-5075. https://doi.org/10.1103/PhysRevLett.74.5072.

[35] H. Trinkaus, Dynamics of viscoelastic flow in ion tracks: origin of plastic deformation of amorphous materials, Nuclear Instruments and Methods in Physics Research B 146 (1998), 204-216. https://doi.org/10.1016/S0168-583X(98)00423-6.

[36] M. Piccardo, F. Bosia, P. Olivero, N. Pugno, An analytical model for the mechanical deformation of locally graphitized diamond, Diamond & Related Materials 48 (2014), 73–81. http://dx.doi.org/10.1016/j.diamond.2014.07.006.

Captions

Fig. 1. Electronic (dots) and nuclear (triangles) energy loss vs. depth in an Er:tungsten-tellurite glass irradiated with 11 MeV C^{4+} ions. Note that nuclear energy loss was multiplied by 10 for better visibility.

Fig. 2. Interference phase contrast micro photo of sections of four channel waveguides written in the Er:tungsten-tellurite glass with a focused beam of 11 MeV C^{4+} ions. Irradiated fluence of the lowermost channel was $4.6 \cdot 10^{14}$ ion/cm^2, and $1.4 \cdot 10^{14}$ ion/cm^2 for the others.

Fig. 3. Propagation, insertion and coupling losses vs. temperature of the 30-minute stepwise annealing step measured at λ = 1400 nm in a 9 mm long channel waveguide written with a 11 MeV C^{4+} ion microbeam at a fluence of $4.6 \cdot 10^{14}$ ion/cm^2. The lines are only an aid to the eye.

Fig. 4. Micro photo of the mode profile of the tested channel waveguide. Irradiated fluence was $4.6 \cdot 10^{14}$ ion/cm^2. Annealing 150 °C, 30 minutes. Measurement was performed at λ = 1400 nm.

Fig. 5. Dimension of the guided mode as a function of the annealing temperature. Fluence = $4.6 \cdot 10^{14}$ ion/cm^2.

Fig. 6. Surface profile of three channel waveguides after stepwise thermal annealing up to 300 °C. E= 11 MeV. Irradiated fluences from left to right: $1.4 \cdot 10^{14}$ ion/cm^2, $1.4 \cdot 10^{14}$ ion/cm^2 and $4.6 \cdot 10^{14}$ ion/cm^2.

Fig. 7. Full width at half maximum of the 922.3 cm^{-1} Raman line across a channel waveguide, irradiated with a carbon microbeam of E= 11 MeV at a fluence of $4.6 \cdot 10^{15}$ ion/cm^2 and annealed thermally.

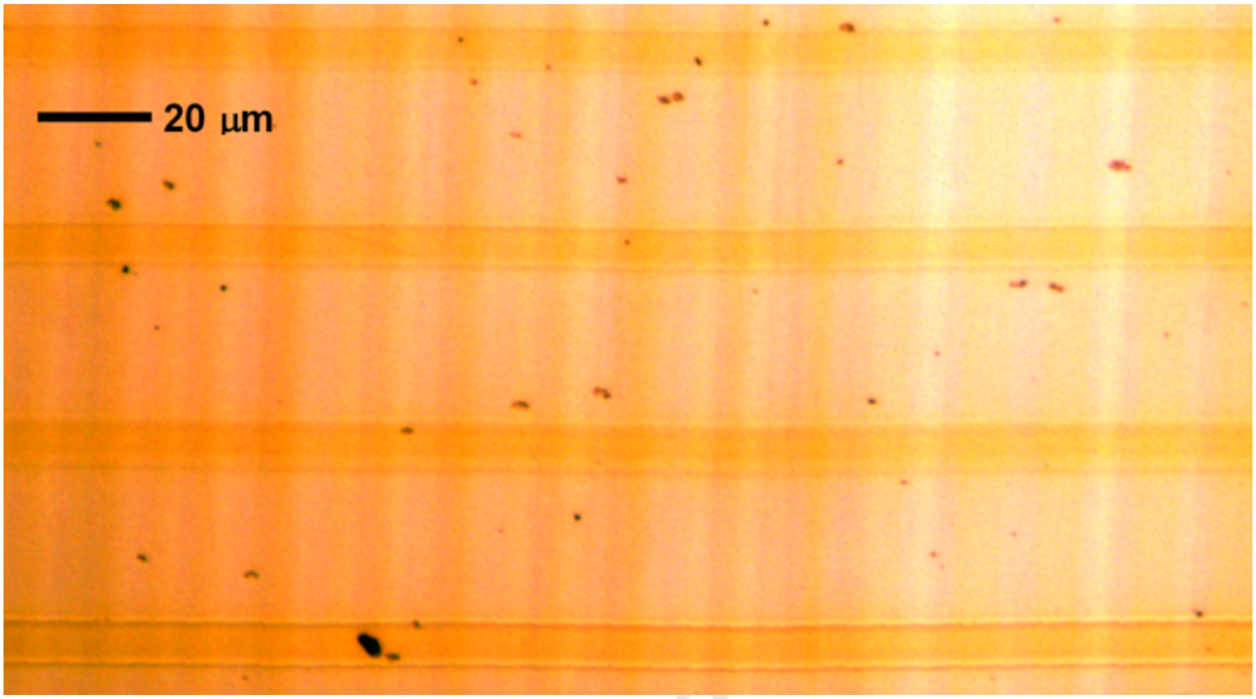
20 μm

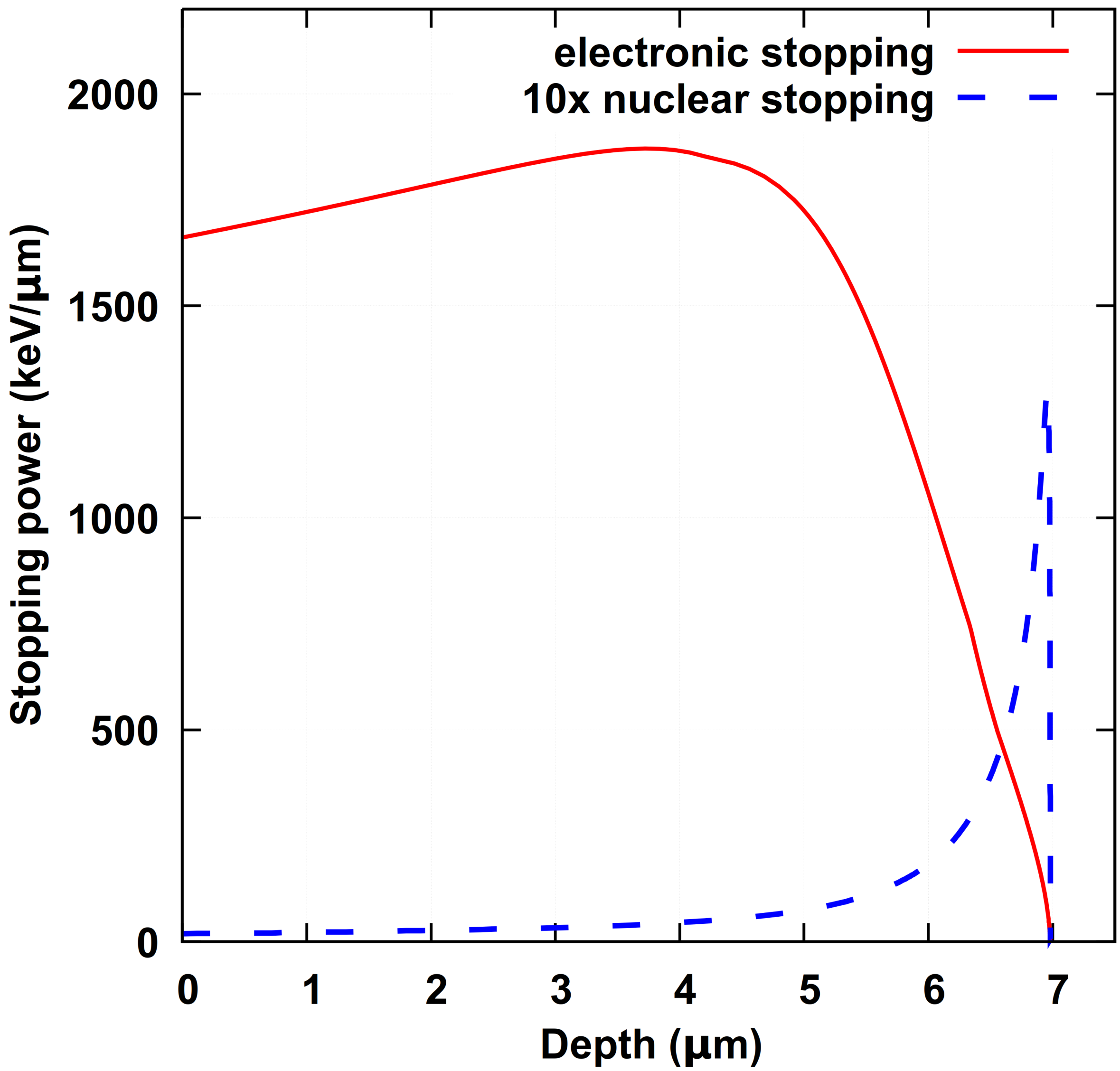
electronic stopping
10x nuclear stopping
2000
1500
1000
500
0
Stopping power (keV/µm)
0
1
2
3
4
5
6
7
Depth (µm)

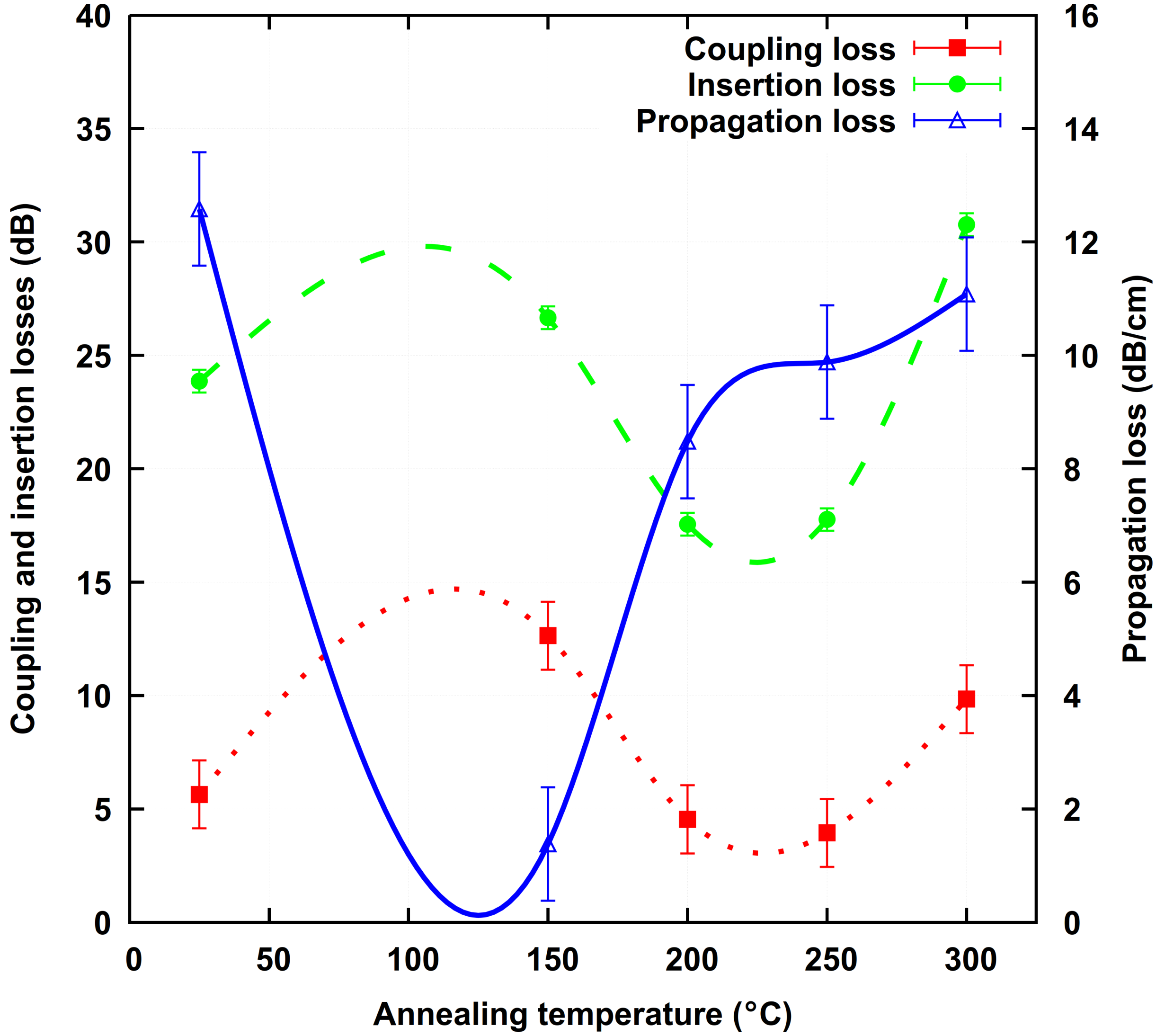
Coupling loss
Insertion loss
Propagation loss
Coupling and insertion losses (dB)
Propagation loss (dB/cm)
Annealing temperature (°C)
0
50
100
150
200
250
300
0
5
10
15
20
25
30
35
40
0
2
4
6
8
10
12
14
16

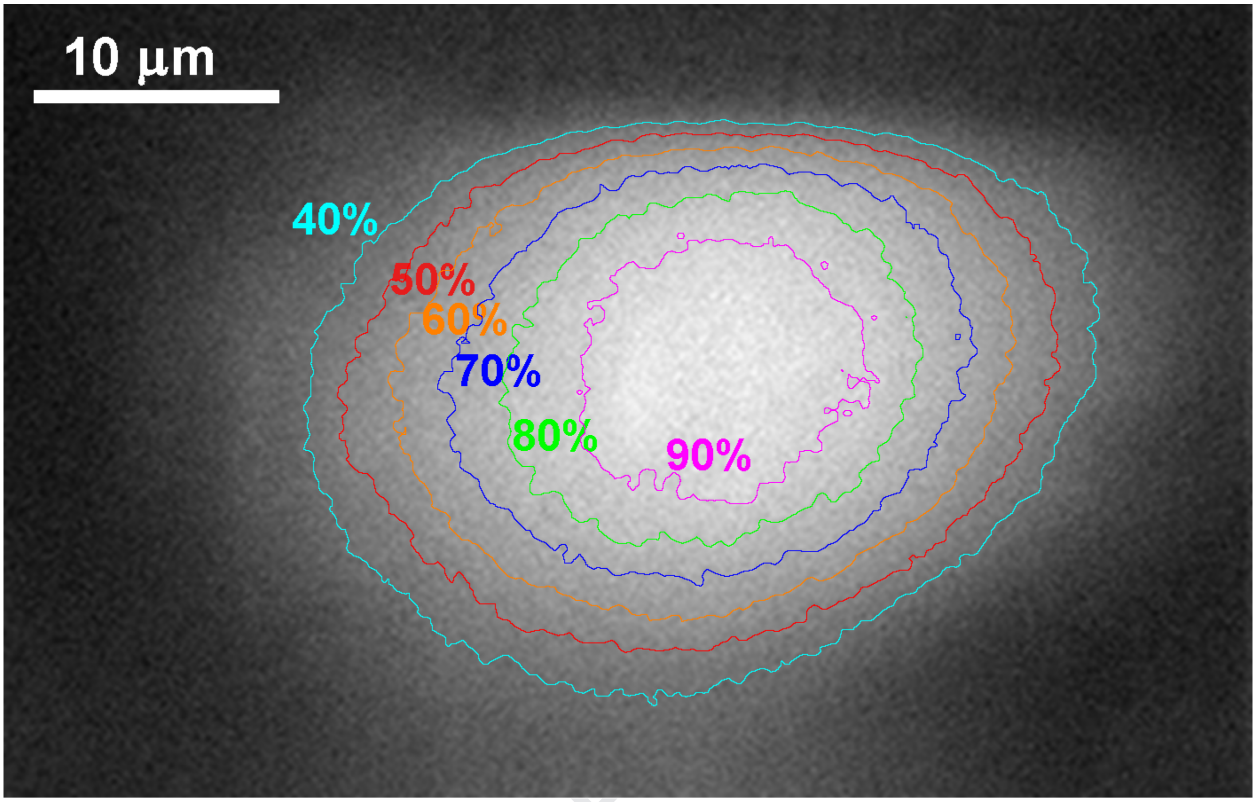
10 µm
40%
50%
60%
70%
80%
90%

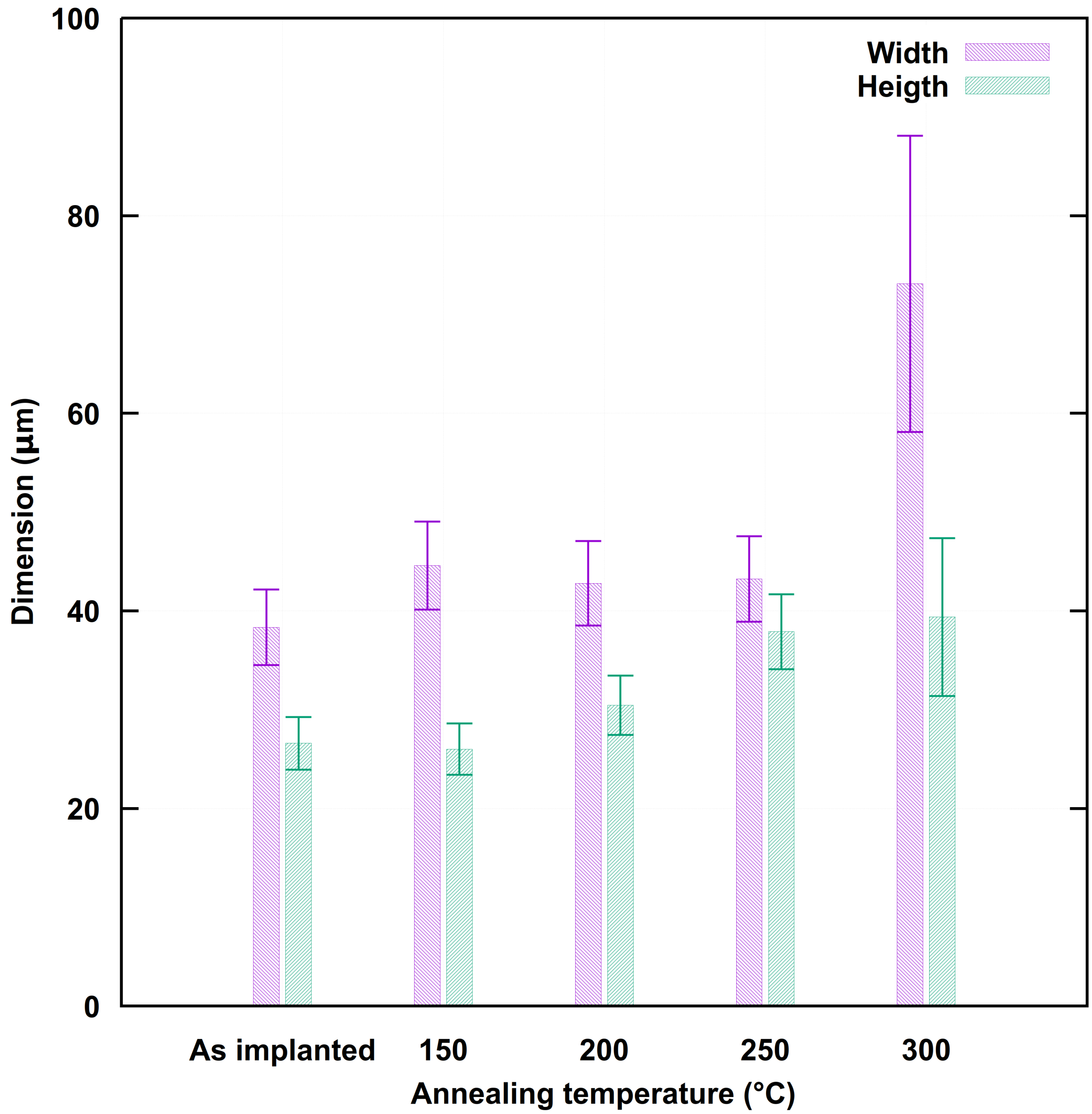

100
80
60
40
20
0
Dimension (µm)
Width
Heigth
As implanted
150
200
250
300
Annealing temperature (°C)

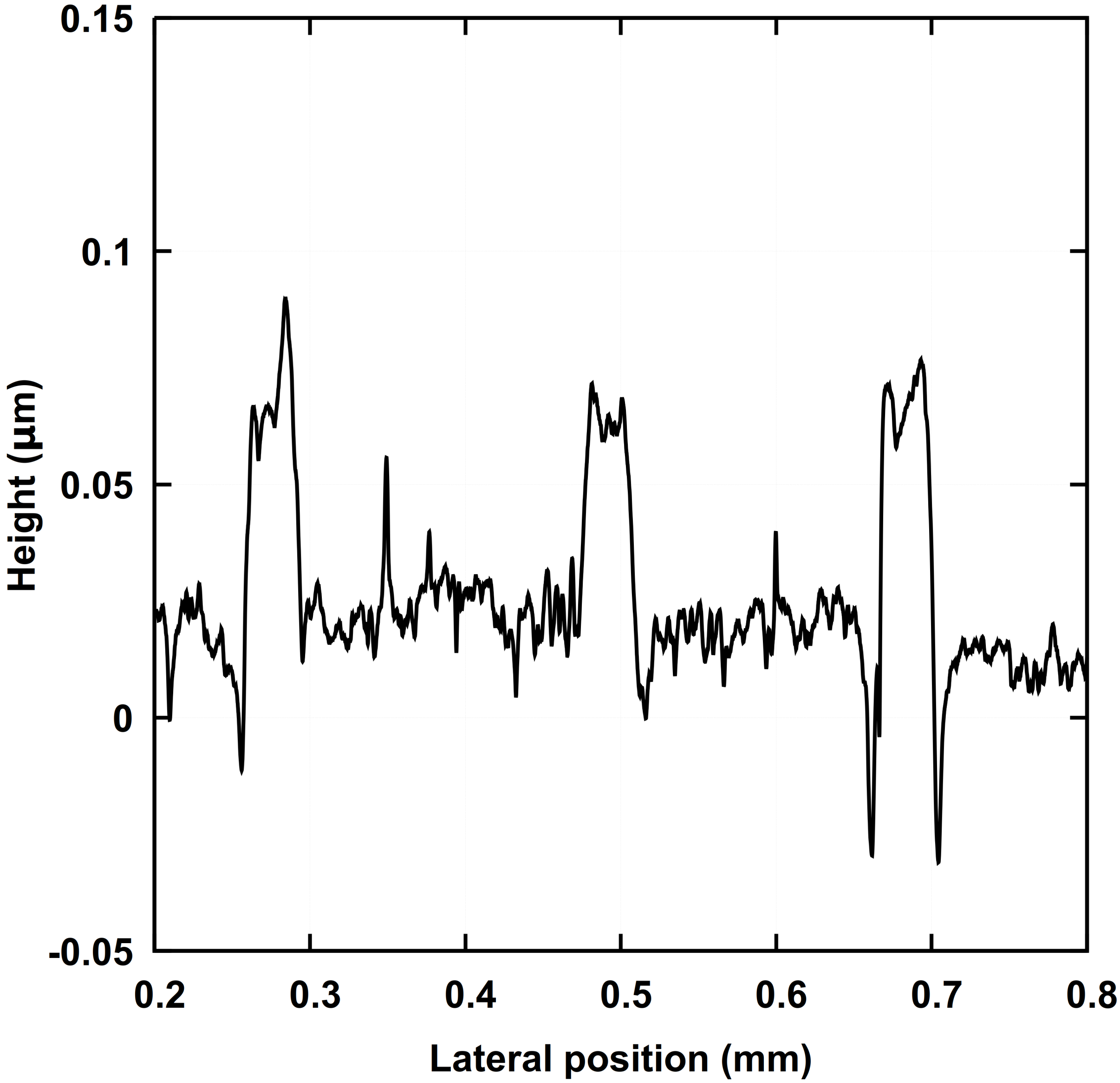
0.15
0.1
0.05
0
-0.05
Height (µm)
0.2
0.3
0.4
0.5
0.6
0.7
0.8
Lateral position (mm)

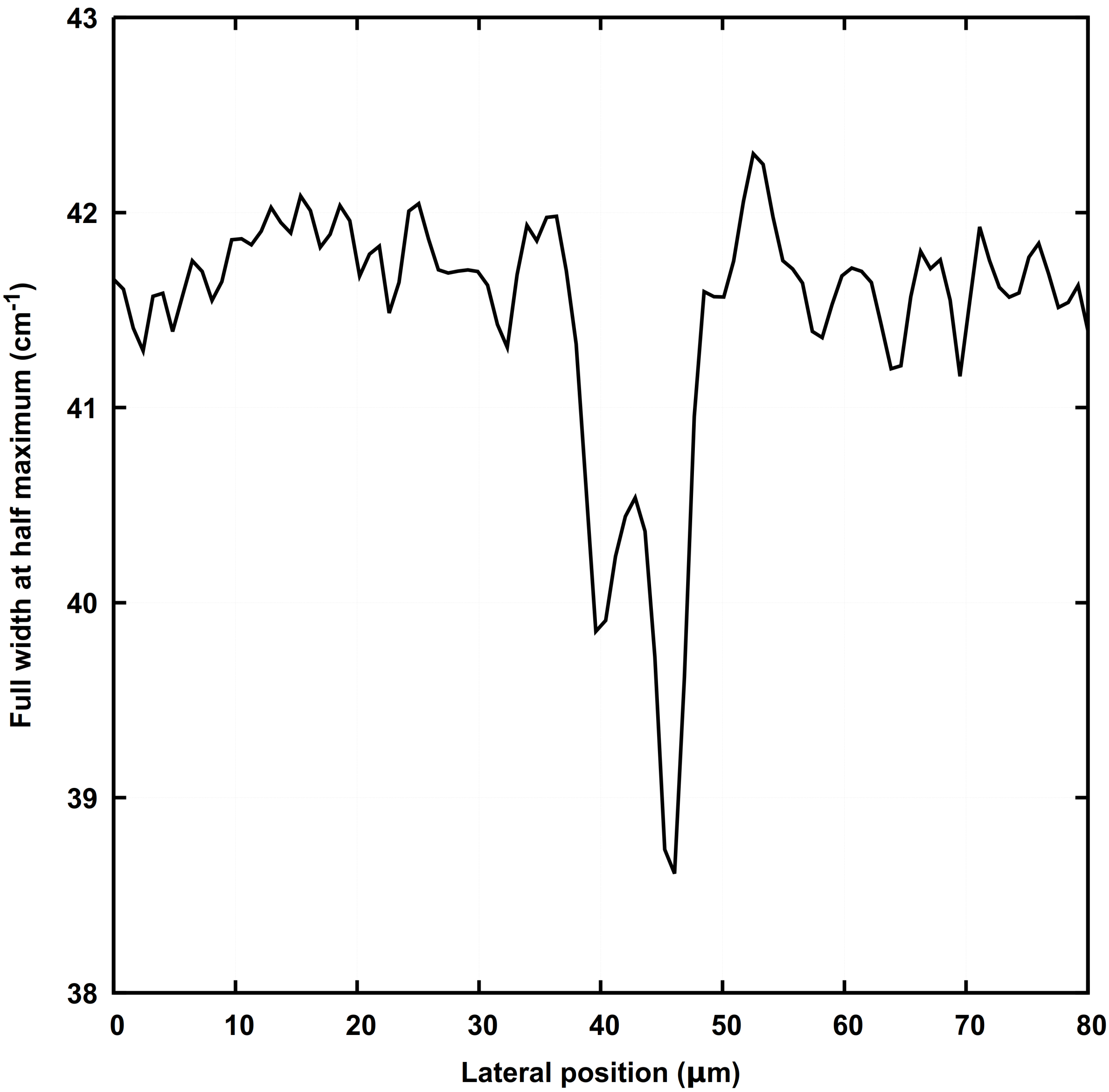

Full width at half maximum (cm^{-1})
43
42
41
40
39
38
0
10
20
30
40
50
60
70
80
Lateral position (µm)

Highlights

- Optical channel waveguides produced by C^{4+} ion microbeam.
- Swift heavy ions produce waveguides with fluences lower than those required with low energy ions→ shorter irradiation times.
- Use of ion microbeam allows direct writing of channel waveguides → no need of photolithograpy.
- Annealing process decreases propagation losses to 1.5 dB/cm at 1400 nm.

Declaration of interests

X The authors declare that they have no known competing financial interests or personal relationships that could have appeared to influence the work reported in this paper.

DThe authors declare the following financial interests/personal relationships which may be considered as potential competing interests: